

Karolinska Institutet

CMM CENTER FOR MOLECULAR MEDICINE

**Fluorescentna mikroskopija.
Tehnike oslikavanja, poboljšanje rezolucije
zaobilaženjem difrakcione barijere i izučavanje
dinamičkih procesa**

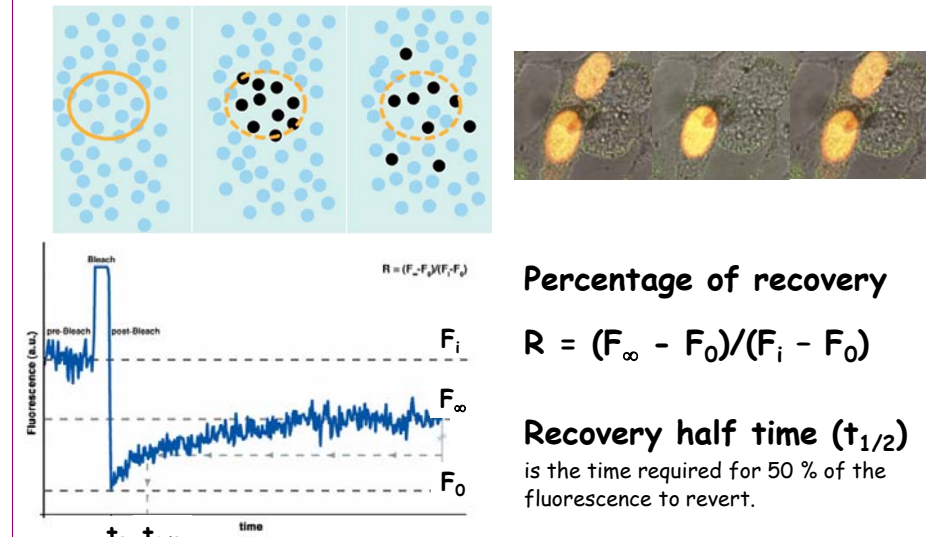
Dr Vladana Vukojević, Associate Professor
Karolinska Institutet, Department of Clinical Neuroscience (CNS)
Center for Molecular Medicine (CMM), Stockholm, Sweden

Fakultet za fizičku hemiju, Univerzitet u Beogradu
29. juni, Beograd, Srbija

Outline

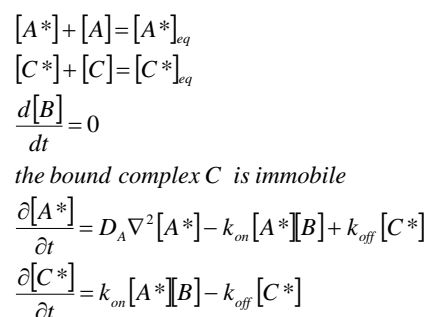
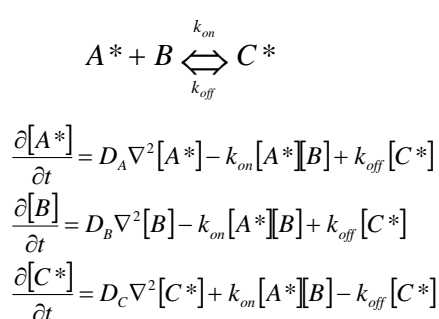
- Quantitative study of molecular interactions and mobility in live cells
 - Fluorescence Recovery After Photobleaching (FRAP)
 - Förster Resonance Energy Transfer (FRET)
 - Fluorescence Lifetime Imaging Microscopy (FLIM)
 - Fluorescence Correlation Spectroscopy (FCS)
 - Raster Image Correlation Spectroscopy (RICS)
 - Quantitative Confocal Laser Scanning Microscopy via massively parallel FCS (mpFCS)

Fluorescence Recovery After Photobleaching (FRAP)



<http://www.science.mcmaster.ca/biochem/faculty/truant/videos.htm>; <http://www.embl.de/eamnet/frap/FRAP6.html>
<http://www.biophysj.org/cgi/content/full/86/6/3473>; <http://www.youtube.com/watch?v=bhjP9PqfJRE>

FRAP is governed by diffusion and chemical kinetics



$\nabla^2 = \frac{\partial^2}{\partial x^2} + \frac{\partial^2}{\partial y^2} + \frac{\partial^2}{\partial z^2}$ - the Laplace operator (Laplacian)

D - diffusion coefficient for each of the three species

k_{on} - kinetic rate constant of the forward reaction

k_{off} - kinetic rate constant of the backward reaction

Sprague BL, Pego RL, Stavreva DA, McNally JG. Analysis of Binding Reactions by Fluorescence Recovery after Photobleaching. *Biophys J* (2004) **86**: 3473-3495

Diffusion dominant FRAP

$$D = \frac{\pi^2}{4 \cdot t_{1/2}}$$

ω - width of the beam

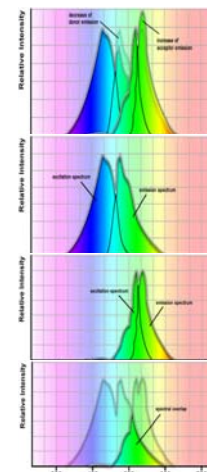
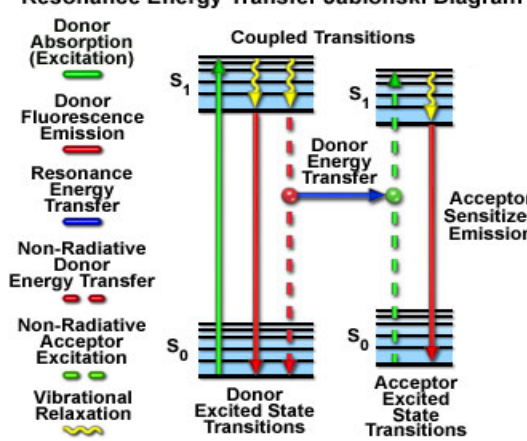
Percentage of FRAP recovery (R) reflects the abundance of the immobile fraction.

Reaction dominant FRAP

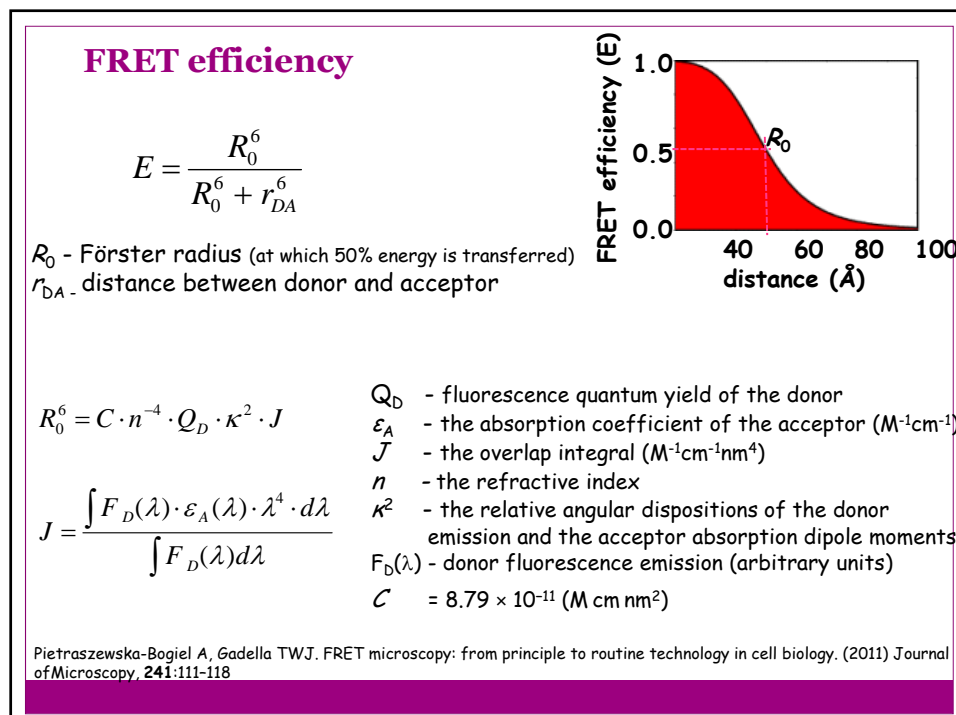
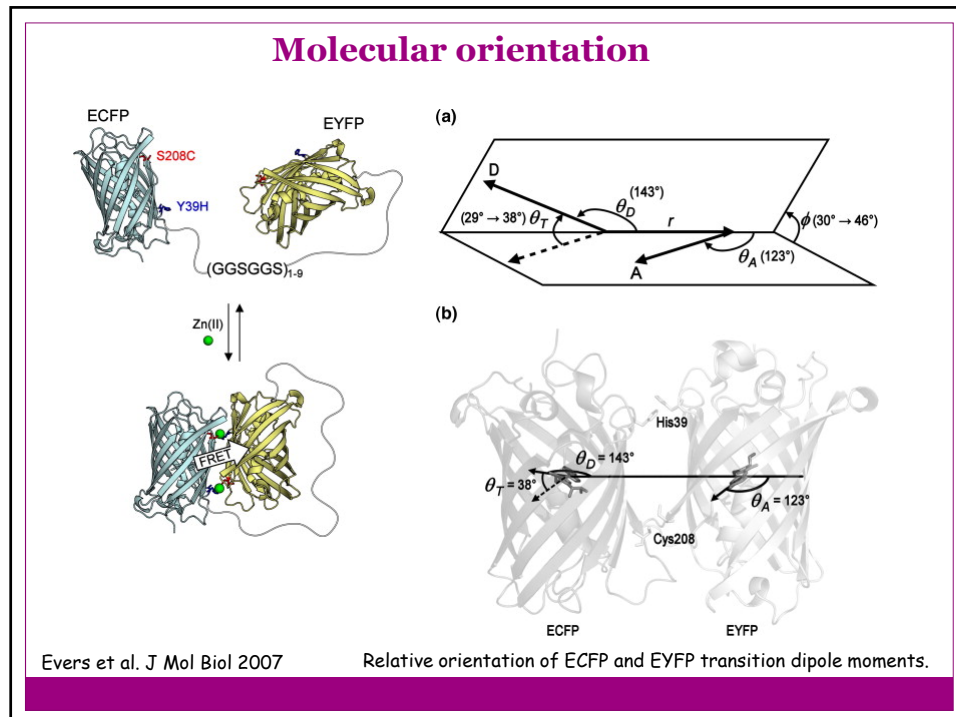
$$\begin{aligned} FRAP(t) &= 1 - [C^*]_{eq} \cdot e^{k_{off}t} \\ [A^*]_{eq} + [C^*]_{eq} &= 1 \end{aligned}$$

Förster Resonance Energy transfer (FRET)

Resonance Energy Transfer Jablonski Diagram

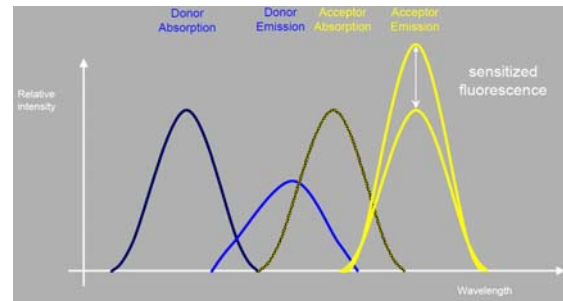


In biological studies, the most often applied genetic probes pair is the CFP-YFP. The R_0 distance for the CFP-YFP pair reported in various studies is 4.5 - 7.0 nm.



FRET effect on donor and acceptor emission spectra

Donor (Em.)	Acceptor (Exc.)
FITC (520 nm)	TRITC (550 nm)
Cy3 (566 nm)	Cy5 (649 nm)
EGFP(508 nm)	Cy3 (554 nm)
CFP (477 nm)	YFP (514 nm)
EGFP (508 nm)	YFP (514 nm)



FRET measuring techniques

• **Intensity-based**

• **Acceptor photobleaching (irreversible photodestruction of acceptor absorption)**

• **Donor photobleaching**

• **FRET via fluorescence lifetime measurements**

$$\begin{aligned} E &= 1 - \frac{Q_{DA}}{Q_D} = 1 - \frac{I_{DA}}{I_D} = 1 - \frac{\tau_{DA}}{\tau_D} = 1 - \frac{\tau_{bl,D}}{\tau_{bl,DA}} = \\ &= \frac{\varepsilon_A}{\varepsilon_D} \cdot \left(\frac{SE}{I_A} \right) = \frac{\varepsilon_A}{\varepsilon_D} \cdot \left(\frac{I_{AD}}{I_A} - 1 \right) \end{aligned}$$

Q_{DA} - quantum yield of the donor in the **presence** of the acceptor

Q_D - quantum yield of the donor in the **absence** of the acceptor

I_{DA} - fluorescence emission intensity of the donor in the **presence** of the acceptor

I_D - fluorescence emission intensity of the donor in the **absence** of the acceptor

τ_{DA} - fluorescence lifetime of the donor in the **presence** of the acceptor

τ_D - fluorescence lifetime of the donor in the **absence** of the acceptor

$\tau_{bl,DA}$ - donor photobleaching time in the **presence** of the acceptor

$\tau_{bl,D}$ - donor photobleaching time in the **absence** of the acceptor

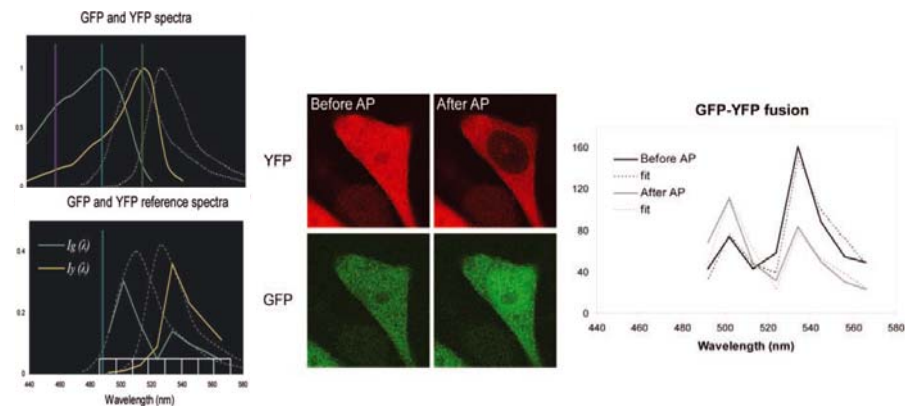
SE - sensitized emission, increased acceptor fluorescence emission intensity (I)

ε - molar absorption coefficient

FRET by acceptor photobleaching

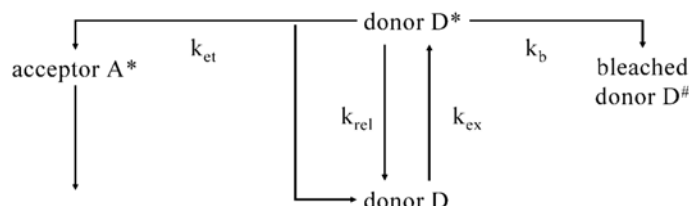
FRET by acceptor photobleaching measures the difference in donor fluorescence intensity in the sample before and after destroying the acceptor by photobleaching:

$$FRET_{\text{eff}} = (D_{\text{post}} - D_{\text{pre}})/D_{\text{post}}$$



Dinant et al. J Microscopy 2008; <http://onlinelibrary.wiley.com/doi/10.1111/j.1365-2818.2008.02020.x/pdf>
http://bti.cornell.edu/pdfs/PCIC_Manuals/AppNote_FRET_AB.pdf

FRET by donor photobleaching

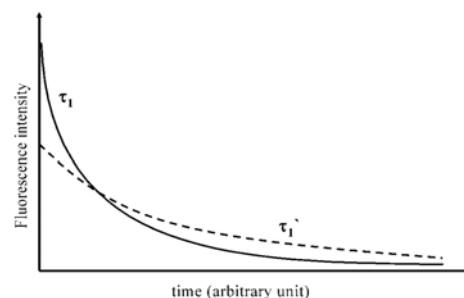


$$E = k_{et}/(k_{rel} + k_{et}) = 1 - \frac{\tau_{dd}}{\tau_d}$$

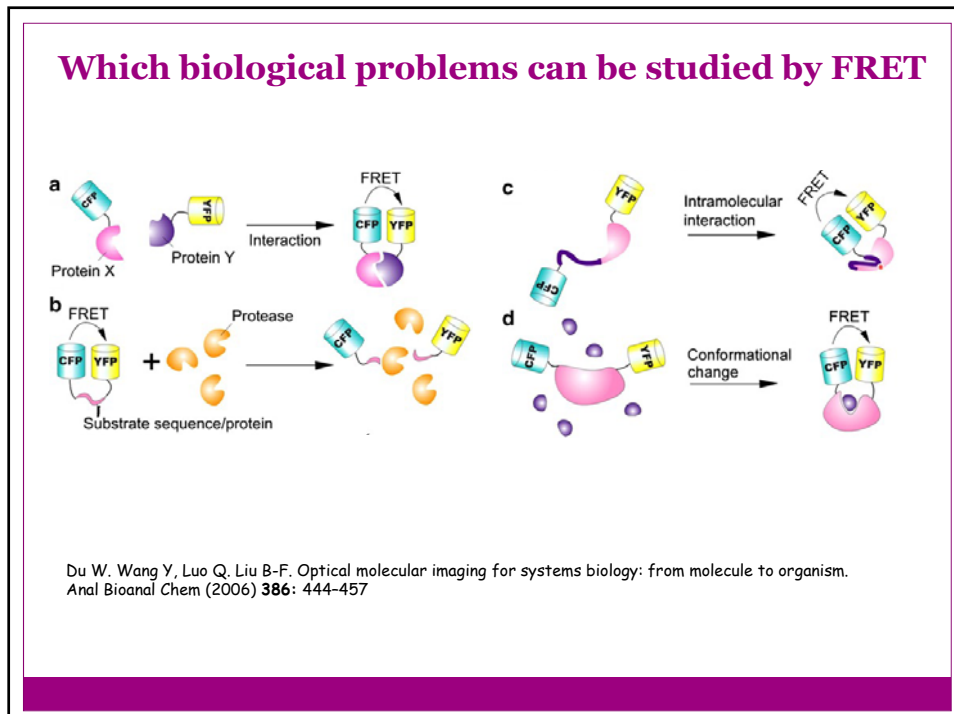
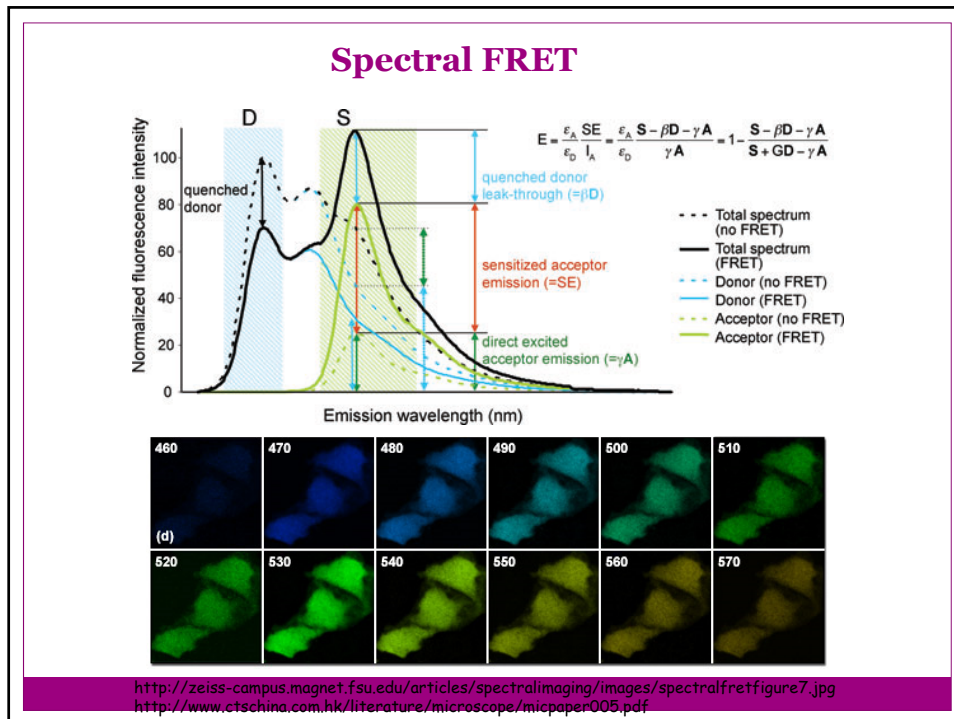
$$\tau_1 \approx (k_{rel})/(k_{ex}k_b)$$

$$\tau'_1 \approx (k_{et} + k_{rel})/(k_{ex}k_b)$$

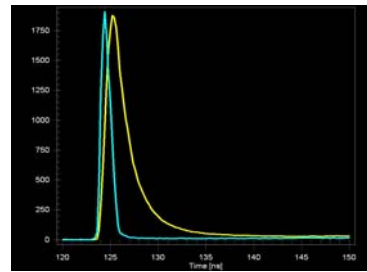
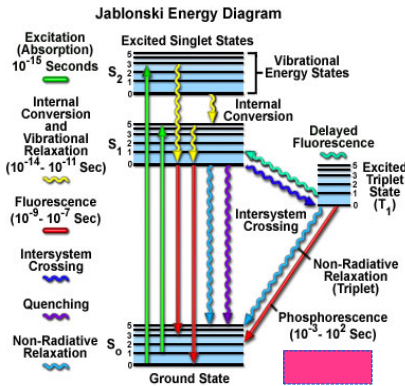
$$E = 1 - \tau_1/\tau'_1$$



Szentesi et al. Cytometry A 2005
<http://onlinelibrary.wiley.com/doi/10.1002/cyto.a.20175/pdf>



Fluorescence Lifetime Imaging Microscopy (FLIM)



Fluorescence lifetime, τ , is defined as the time required for the fluorescence intensity to decay by the factor $1/e$.

The experimentally measured lifetime (τ) contains contributions from internal conversion (IC) and intersystem crossing (ISC):

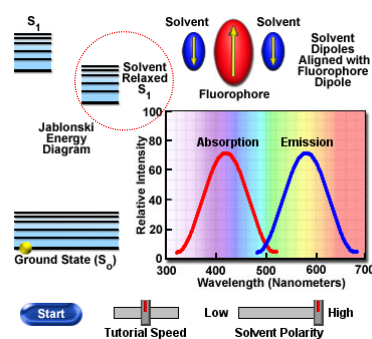
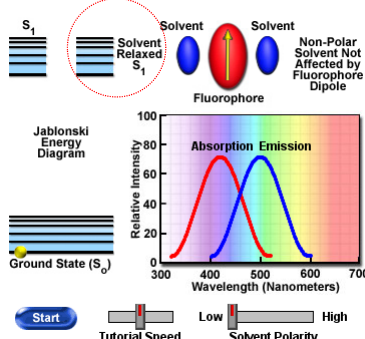
$$\frac{1}{\tau} = k_F + k_{IC} + k_{ISC}$$

$$\tau_0 = \frac{1}{k_F} = \frac{\tau}{Q}$$

The natural lifetime (τ_0) describes the contribution from fluorescence emission only.
 Q is the fluorescence quantum yield.

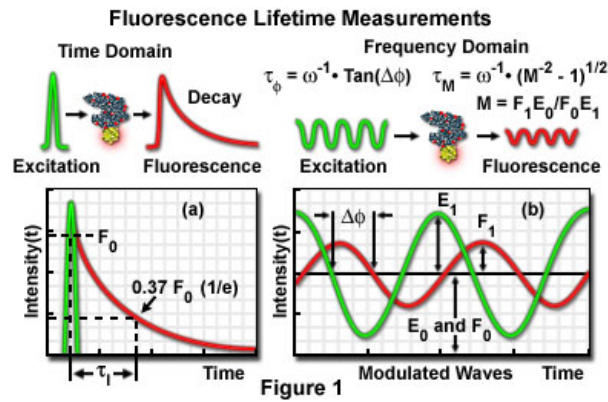
<http://www.olympusconfocal.com/applications/flimintro.html>

Why is fluorescence lifetime changing?



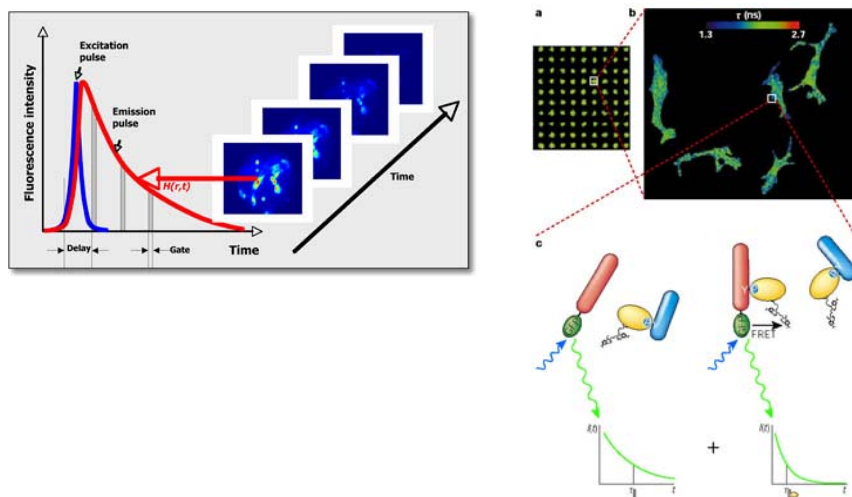
<http://www.olympusmicro.com/primer/java/jablonski/solventeffects/index.html>
<http://pubs.acs.org/doi/pdf/10.1021/ac50036a030>

How can we measure fluorescence lifetime?



<http://www.olympusconfocal.com/applications/flimintro.html>

Examples of FLIM application



Phizicky E, Bastiaens PIH, Zhu H, Snyder M, Fields S. Protein analysis on a proteomic scale. Nature 2003, 422, 208-215

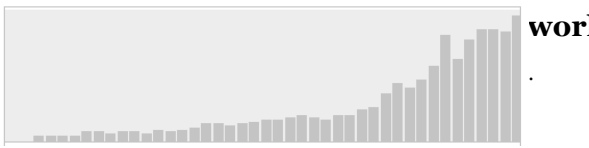
Fluorescence Correlation Spectroscopy (FCS)

Milestones in FCS development

- 1905/1906** Einstein and von Smoluchowski
Fluctuation theory of light scattering
- 1911** Svedberg observed fluctuations in the number of colloidal gold particles under a microscope
- 1913** Perrin anticipated fluorescence fluctuation studies
- 1957** Laser development
- 1957** Confocal microscope
- 1961/1964** Solid state single photon detectors
- 1967** Autocorrelator

Moder

Magde D,
Elson EL,
Ehrenber

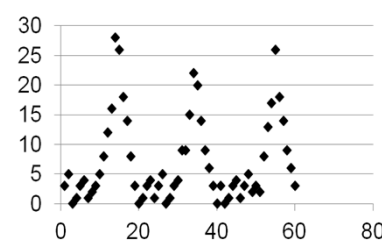


work of

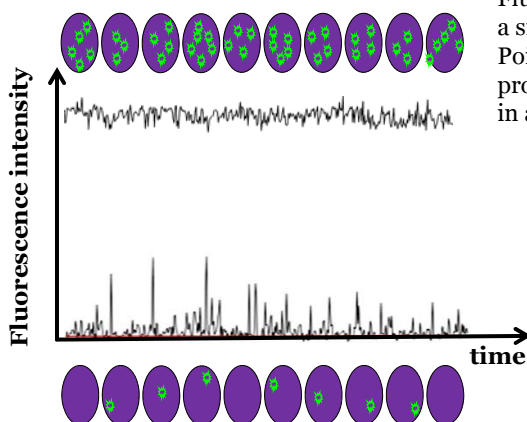
Fluctuation analysis



3 5 0 1 3 4 1 2 3 5 8 12 16 28 26 18 14
8 3 0 1 3 4 1 3 5 0 1 3 4 9 9 15 22 20
14 9 6 3 0 3 0 1 3 4 1 3 5 2 3 2 8 13 17
26 18 14 9 6 3



Fluctuation analysis

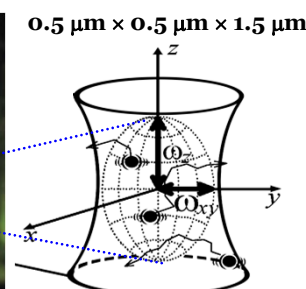
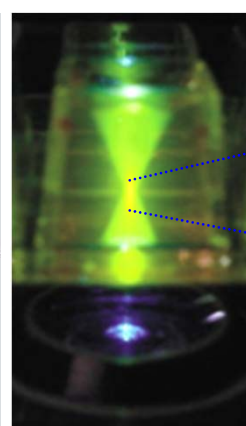
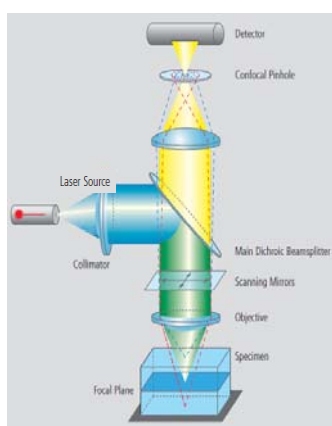


Fluctuations in molecular number in a small volume can be described by a Poisson process, which states that the probability of observing N molecules in a given interval of time is:

$$P(N) = \frac{\langle N \rangle^N e^{-\langle N \rangle}}{N!}$$

$$\frac{1}{N} = \frac{\langle (N - \bar{N})^2 \rangle}{(\bar{N})^2} = \frac{Var}{(\bar{N})^2}$$

FCS coupling with confocal microscopy



Single-molecule sensitivity
Real time analysis
Live cells

[http://www.es.hokudai.ac.jp/
publish/outline/2003/ries14_1.png](http://www.es.hokudai.ac.jp/publish/outline/2003/ries14_1.png)

Fluorescence intensity distribution in the OVE

$$F(t) = \int_V I_{exc}(\vec{r}) \cdot Q(\vec{r}) \cdot S(\vec{r}) \cdot c(\vec{r}, t) dV$$

- I_{exc} - laser intensity profile
- Q - quantum yield of the fluorophore
- S - photon detection sensitivity of the instrument
- c - concentration of the fluorophore

By combining all terms that characterize fluorescence emission and detection, and by assuming that the spatial distribution of the emitted light can be approximated by a three-dimensional Gaussian:

$$W(r) = e^{-\frac{-2x^2 + y^2}{r_0^2}} \cdot e^{-\frac{-2z^2}{z_0^2}}$$

which decays to $1/e^2$ at r_0 in the lateral direction and for $z = z_0$ in the axial direction, fluorescence intensity distribution across the observation volume element can be described as:

$$F(t) = \int_V W(\vec{r}) \cdot c(\vec{r}, t) dV$$

By substituting $F(t)$ in the autocorrelation function and considering only free 3D diffusion:

$$\langle \delta c(\vec{r}, 0) \cdot \delta c(\vec{r}', \tau) \rangle = \langle c \rangle \cdot \frac{1}{(4\pi D \tau)^{\frac{3}{2}}} \cdot e^{-\frac{(\vec{r} - \vec{r}')^2}{4D\tau}}$$

the autocorrelation function for a single, freely diffusing species of molecules:

$$G(\tau) = \frac{1}{V_{eff} \langle c \rangle} \cdot \frac{1}{1 + \frac{\tau}{\tau_D}} \cdot \frac{1}{\sqrt{1 + \left(\frac{r_0}{z_0}\right)^2 \cdot \frac{\tau}{\tau_D}}}$$

$$G(0) = \frac{1}{V_{eff} \langle c \rangle} = \frac{1}{\langle N \rangle} \quad \tau_D = \frac{r_0^2}{4D}$$

$$D = \frac{k \cdot T}{6\pi\eta_v R_h} \quad \frac{1}{D} \propto \frac{6\pi\eta}{kT} \cdot \sqrt[3]{M}$$

Schwille P, Haustein E. Fluorescence Correlation Spectroscopy. An Introduction to its Concepts and Applications. Biophysics Textbook Online 2004

$$\frac{\partial \delta C(\mathbf{r}, t)}{\partial t} = D \nabla^2 \delta C(\mathbf{r}, t)$$

$$\delta C(\mathbf{r}, t) = \int d\mathbf{p} e^{i\mathbf{p} \cdot \mathbf{r}} \delta C_f(\mathbf{p}, t)$$

$$\frac{\partial \delta C(\mathbf{r}, t)}{\partial t} = \int d\mathbf{p} e^{i\mathbf{p} \cdot \mathbf{r}} \left\{ -D \rho^2 \delta C_f(\mathbf{p}, t) \right\}$$

$$\delta C(\mathbf{r}, t) = \int d\mathbf{p} e^{i\mathbf{p} \cdot \mathbf{r}} \left\{ \delta C_f(\mathbf{p}, 0) e^{-D\rho^2 t} \right\}$$

$$\langle \delta C(\mathbf{r}, t) \delta C(\mathbf{r}', 0) \rangle = \int d\mathbf{p} e^{i\mathbf{p} \cdot \mathbf{r}} \left\langle \left\langle \delta C_f(\mathbf{p}, 0) \delta C(\mathbf{r}', 0) \right\rangle \right\rangle e^{-D\rho^2 t}$$

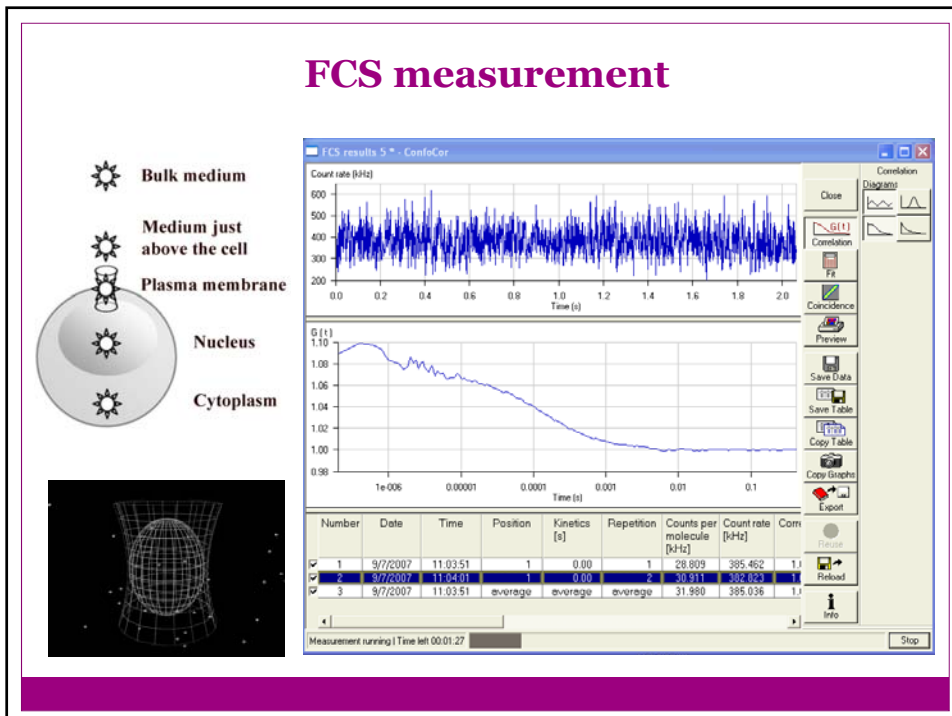
$$= \int d\mathbf{p} e^{i\mathbf{p} \cdot \mathbf{r}} \left\{ \frac{1}{2\pi} \int d\mathbf{r}'' e^{-i\mathbf{p} \cdot \mathbf{r}''} \langle \delta C(\mathbf{r}'', 0) \delta C(\mathbf{r}', 0) \rangle e^{-D\rho^2 t} \right\}$$

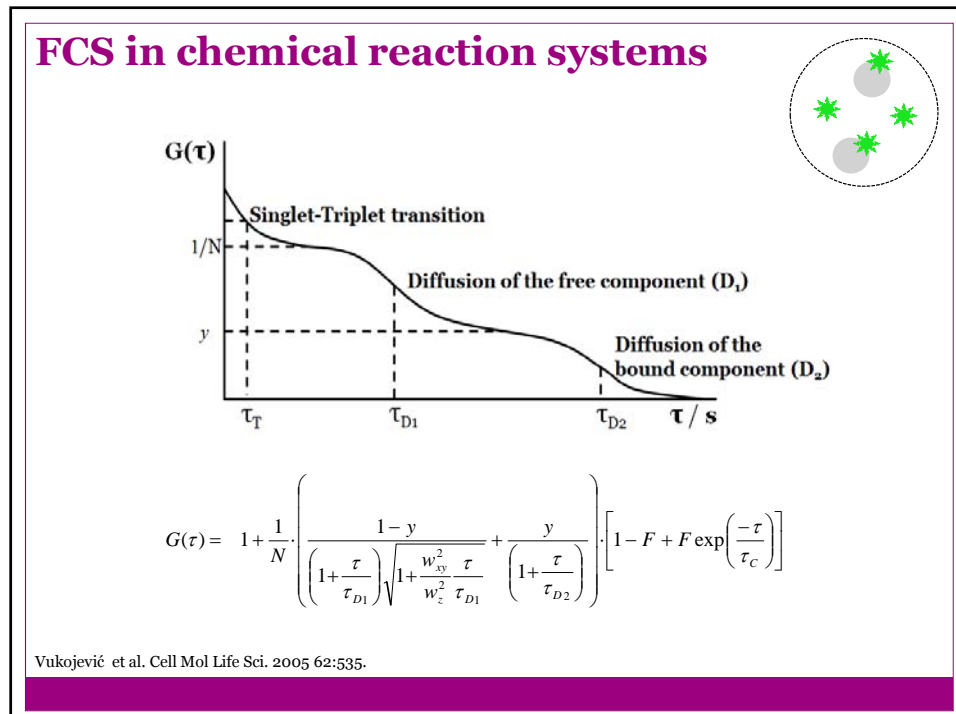
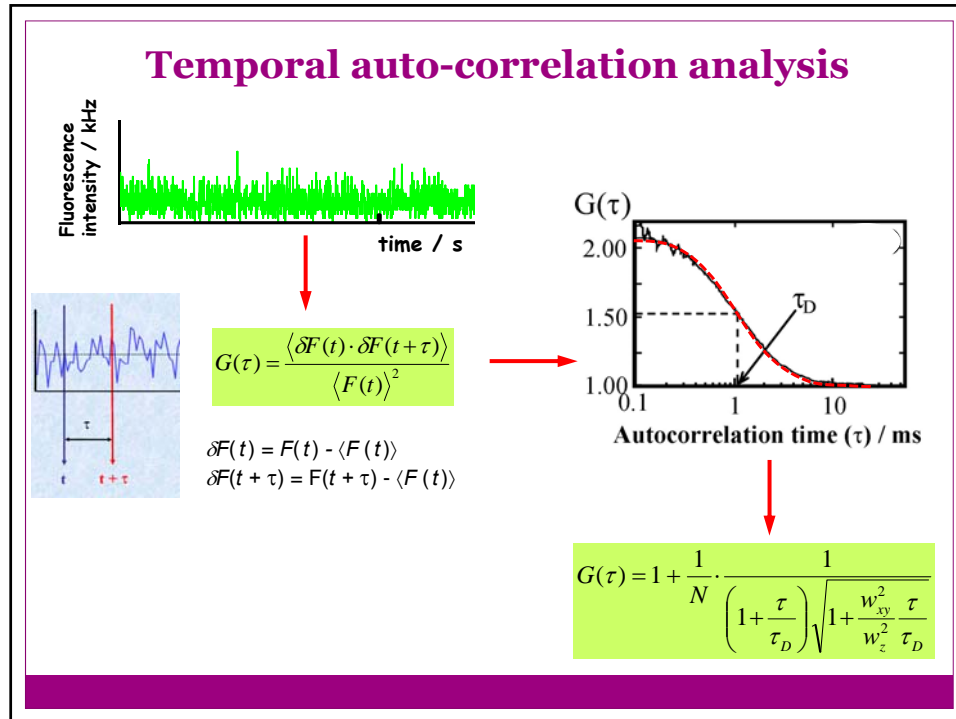
$$= \frac{\langle C \rangle}{2\pi} \int d\mathbf{p} e^{i\mathbf{p} \cdot |\mathbf{r}-\mathbf{r}'| - D\rho^2 t}$$

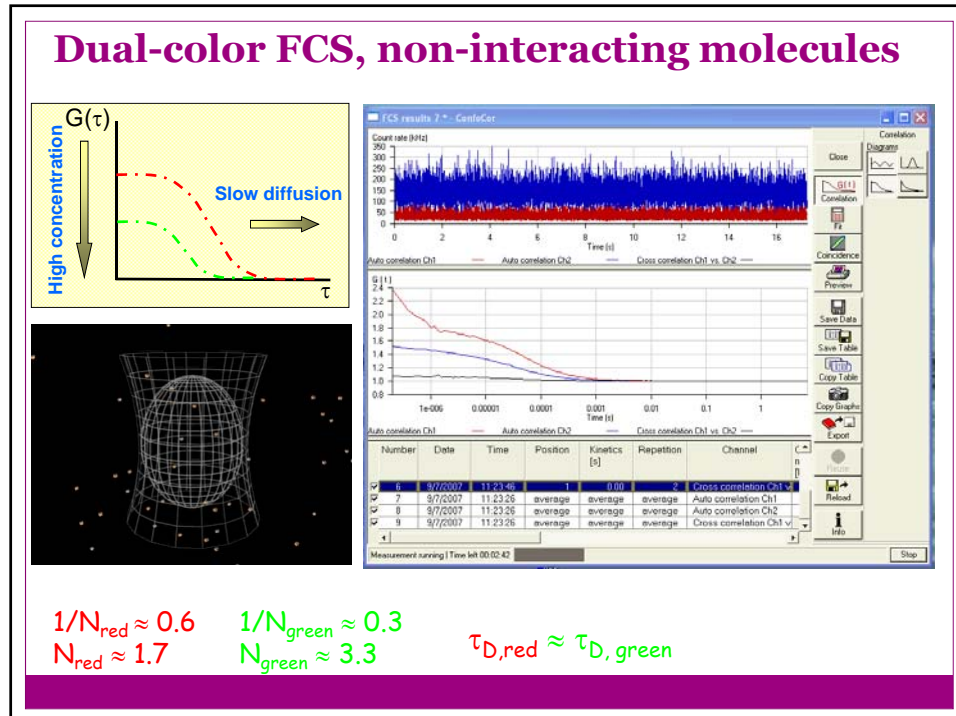
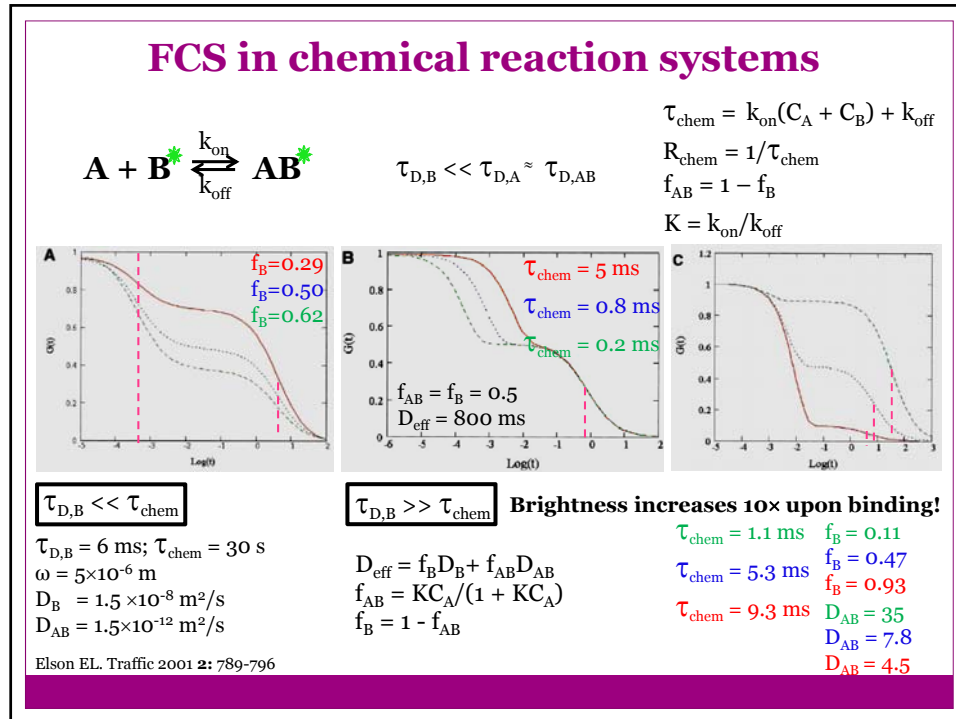
$$\langle \delta C(\mathbf{r}, t) \delta C(\mathbf{r}', 0) \rangle = \frac{\langle C \rangle}{(4\pi Dt)^{\frac{3}{2}}} e^{-\left[\frac{|\mathbf{r}-\mathbf{r}'|^2}{4Dt} \right]}$$

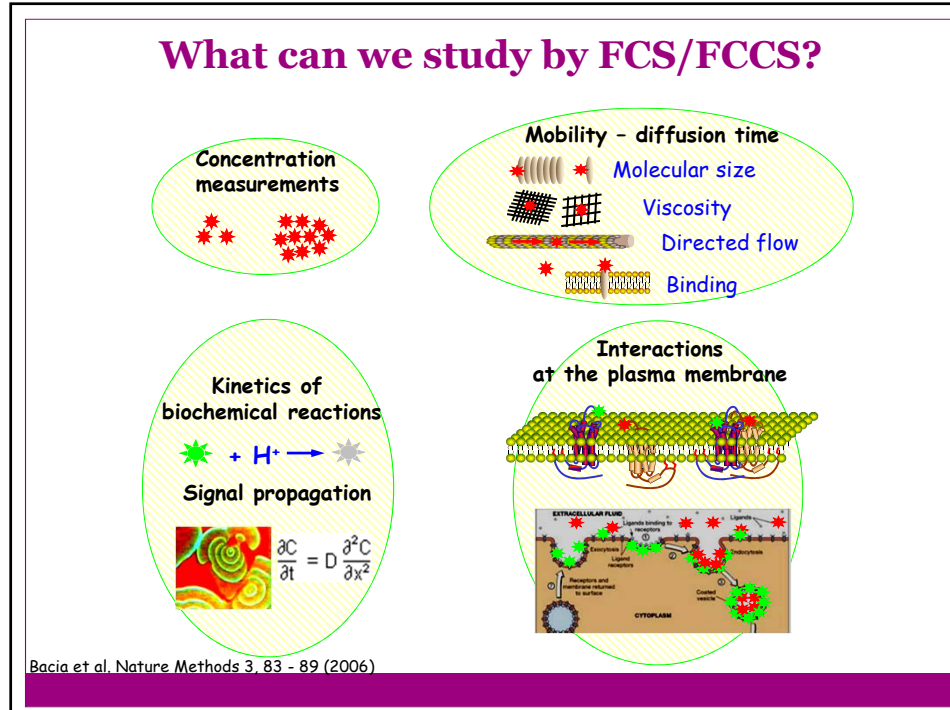
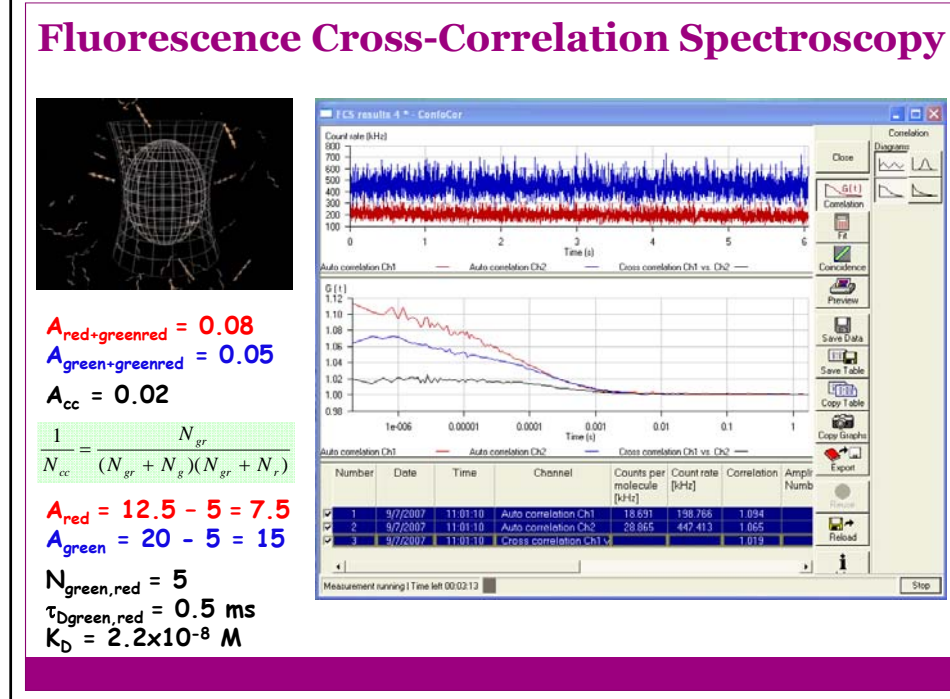
$$G(\tau) = \frac{\iint d\mathbf{r} d\mathbf{r}' W(\mathbf{r}) W(\mathbf{r}') \langle \delta C(\mathbf{r}, \tau) \delta C(\mathbf{r}', 0) \rangle}{[\langle C \rangle \int d\mathbf{r} W(\mathbf{r})]^2} \quad G_D(\tau, N, \tau_D) = \frac{\gamma}{\langle N \rangle} \left(\frac{1}{1 + \tau / \tau_D} \right) \left(\frac{1}{1 + (w_r/w_z)^2 \tau / \tau_D} \right)^{\frac{N}{2}}$$

http://www.cup.uni-muenchen.de/pc/lamb/FCS_Notes/FCS_1.pdf









Examples of autocorrelation functions

AF1 Two-dimensional diffusion of a single fluorescent species

$$G(\tau) = 1 + \frac{1}{N} \cdot \frac{1}{\left(1 + \frac{\tau}{\tau_D}\right)}$$

AF5 Concentration fluctuations around a chemical equilibrium coupled with diffusion

$$G(\tau) = 1 + \frac{1}{N(1-F)} \cdot \frac{1}{\left(1 + \frac{\tau}{\tau_D}\right) \sqrt{1 + \frac{w_{xy}^2}{w_z^2} \frac{\tau}{\tau_D}}} \cdot \left[1 - F + F \exp\left(\frac{-\tau}{\tau_C}\right) \right]$$

The chemical reaction analyzed is $AB \rightleftharpoons A^* + B$; A^* is the only fluorescent species
 F , average fraction of molecules in the non-fluorescent state AB
 τ_C , chemical relaxation time from which rate constants are derived

AF2 Free diffusion of a single species and triplet formation

$$G(\tau) = 1 + \frac{1}{N} \cdot \frac{1}{\left(1 + \frac{\tau}{\tau_D}\right) \sqrt{1 + \frac{w_{xy}^2}{w_z^2} \frac{\tau}{\tau_D}}} \cdot \left[1 + \frac{T}{1-T} \exp\left(-\frac{\tau}{\tau_T}\right) \right]$$

T , average equilibrium fraction of molecules in triplet state
 τ_p , triplet correlation time, related to rate constants for intersystem crossing and t

AF6 Restricted (anomalous) diffusion due to interactions with fixed or mobile structures

$$G(\tau) = 1 + \frac{1}{N} \cdot \frac{1}{\left(1 + \left(\frac{\tau}{\tau_D}\right)^\alpha\right) \sqrt{1 + \frac{w_{xy}^2}{w_z^2} \left(\frac{\tau}{\tau_D}\right)^\alpha}}$$

α , restriction coefficient; for free (Brownian) diffusion $\alpha = 1$, and for restricted diffusion $\alpha < 1$

AF3 Free diffusion of unbound ligand and the ligand-receptor complex

$$G(\tau) = 1 + \frac{1}{N} \cdot \left(\frac{1-y}{\left(1 + \frac{\tau}{\tau_{D_1}}\right) \sqrt{1 + \frac{w_{xy}^2}{w_z^2} \frac{\tau}{\tau_{D_1}}}} + \frac{y}{\left(1 + \frac{\tau}{\tau_{D_2}}\right) \sqrt{1 + \frac{w_{xy}^2}{w_z^2} \frac{\tau}{\tau_{D_2}}}} \right)$$

y , fraction of ligand bound to the receptor
 τ_{D_1} , diffusion time of the unbound ligand
 τ_{D_2} , diffusion time of the bound ligand

AF7 Active transport

$$G(\tau) = 1 + \frac{1}{N} \cdot \exp\left(-\left(\tau \frac{v}{w_{xy}}\right)^2\right)$$

v , velocity of active radial transport

AF4 Free diffusion of unbound ligand and diffusion of a ligand bound to a surface

$$G(\tau) = 1 + \frac{1}{N} \cdot \left(\frac{1-y}{\left(1 + \frac{\tau}{\tau_{D_1}}\right) \sqrt{1 + \frac{w_{xy}^2}{w_z^2} \frac{\tau}{\tau_{D_1}}}} + \frac{y}{\left(1 + \frac{\tau}{\tau_{D_2}}\right) \sqrt{1 + \frac{w_{xy}^2}{w_z^2} \frac{\tau}{\tau_{D_2}}}} \right)$$

y , fraction of bound ligand
 τ_{D_1} , diffusion time of the unbound ligand
 τ_{D_2} , diffusion time of the bound ligand

AF8 Mixed mode diffusion – active transport coupled with diffusion

$$G(\tau) = 1 + \frac{1}{N} \cdot \frac{1}{\left(1 + \frac{\tau}{\tau_D}\right) \sqrt{1 + \frac{w_{xy}^2}{w_z^2} \frac{\tau}{\tau_D}}} \cdot \exp\left(-\left(\tau \frac{v}{w_{xy}}\right)^2 \cdot \left(\frac{1}{\left(1 + \frac{\tau}{\tau_D}\right)}\right)\right)$$

Vukojević et al. Cell Mol Life Sci. 2005 62:535.

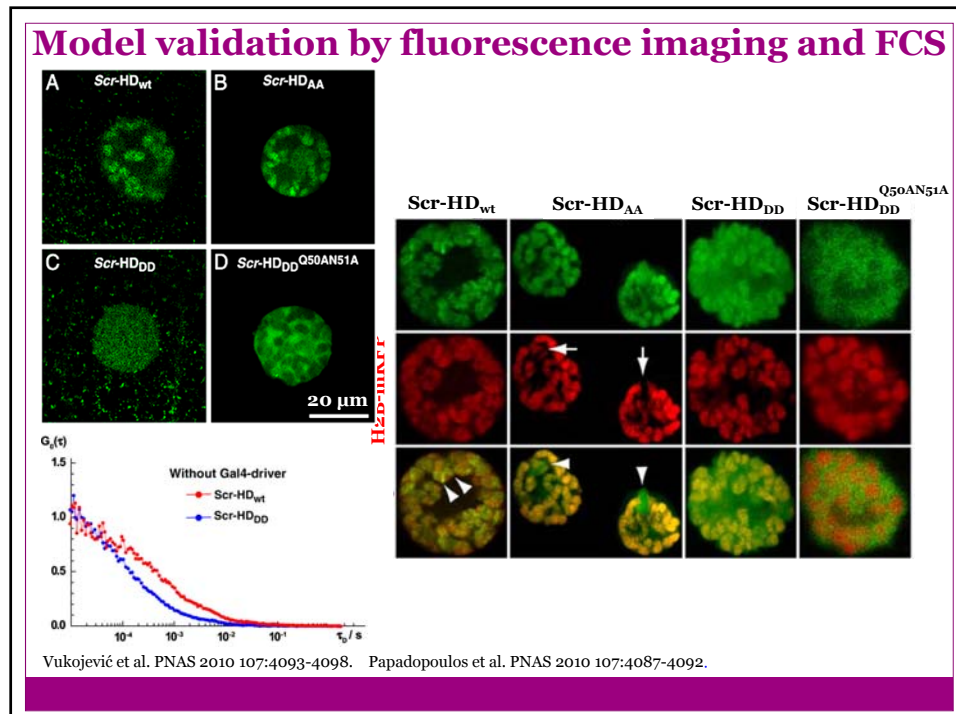
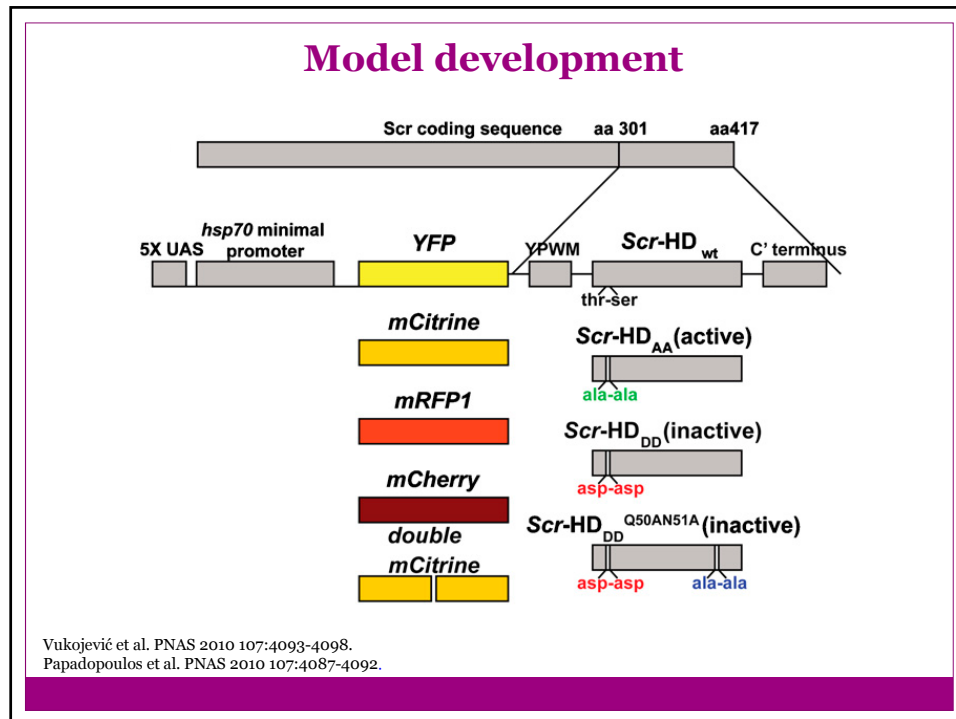
Scr transcription factor

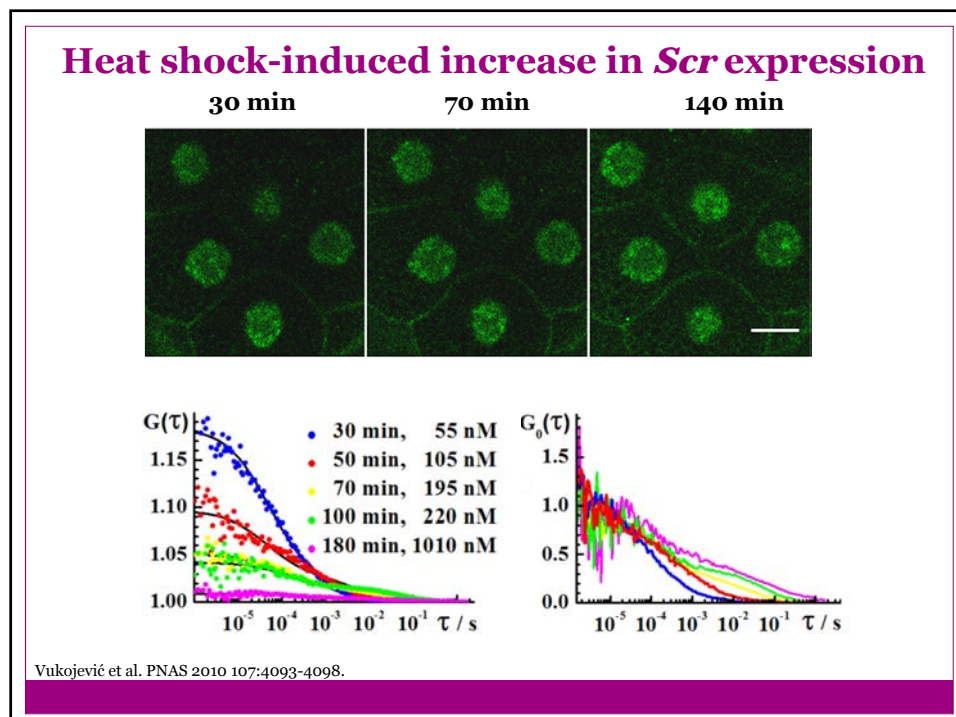
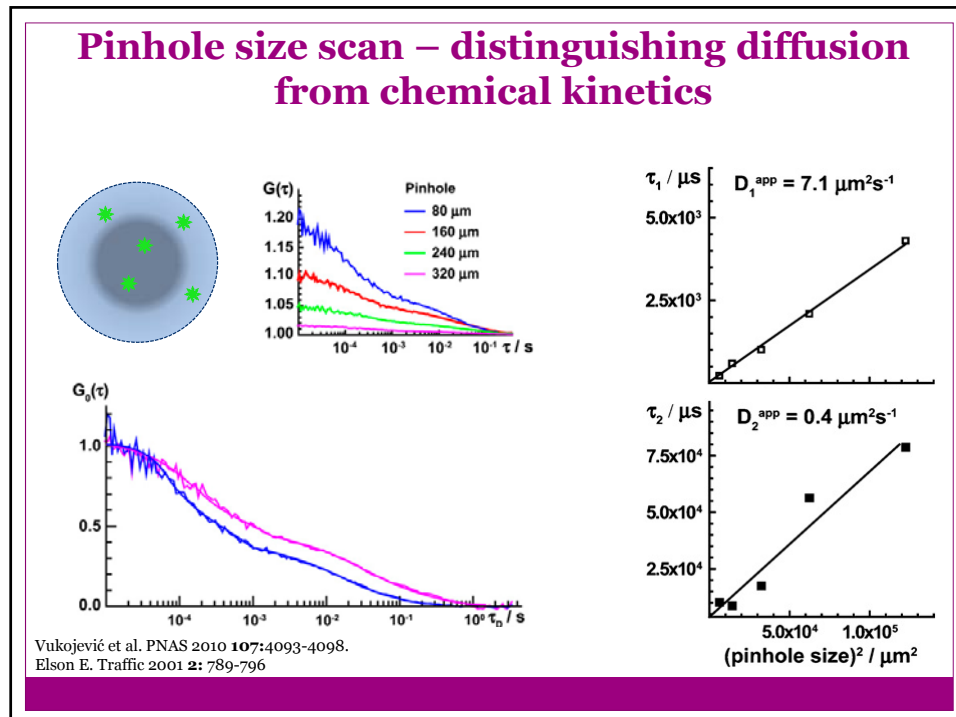
The diagram shows a Drosophila fly with numbered segments (1-13). Above the fly, two gene complexes are shown: Antennapedia complex (lab, Pb, Dfd, Scr, Antp) and bithorax complex (Ubx, AbdA, AbdB). Below the fly, three abdominal segments are detailed: Deformed (Dfd), Sex comb reduced (Scr), Antennapedia (Antp), and Ultrabithorax (Ubx). Each segment is associated with a specific Hox gene from the respective complex.

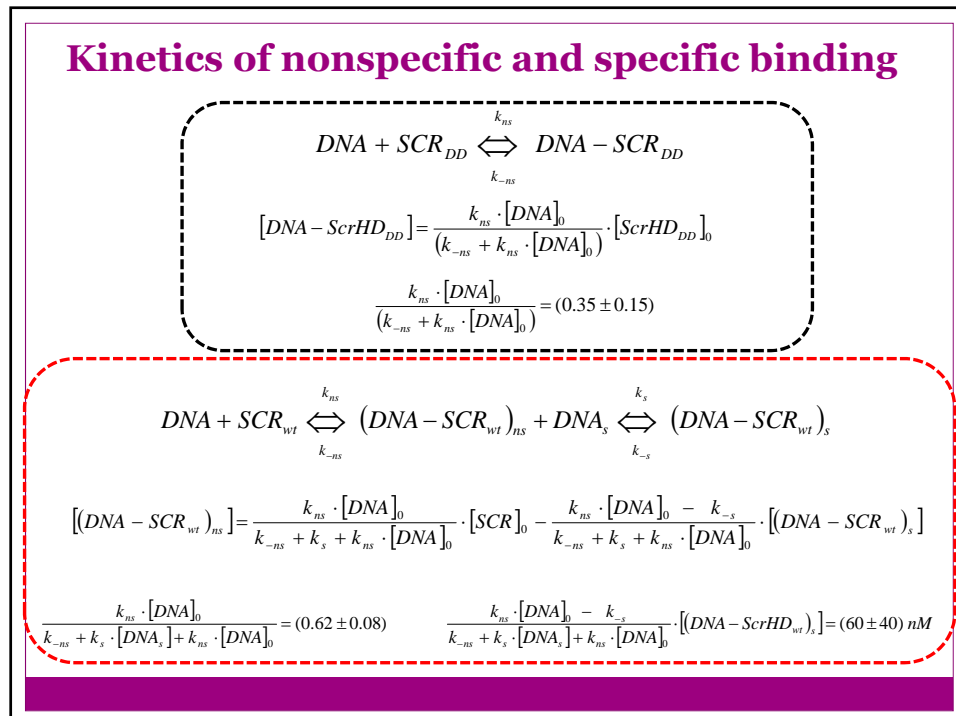
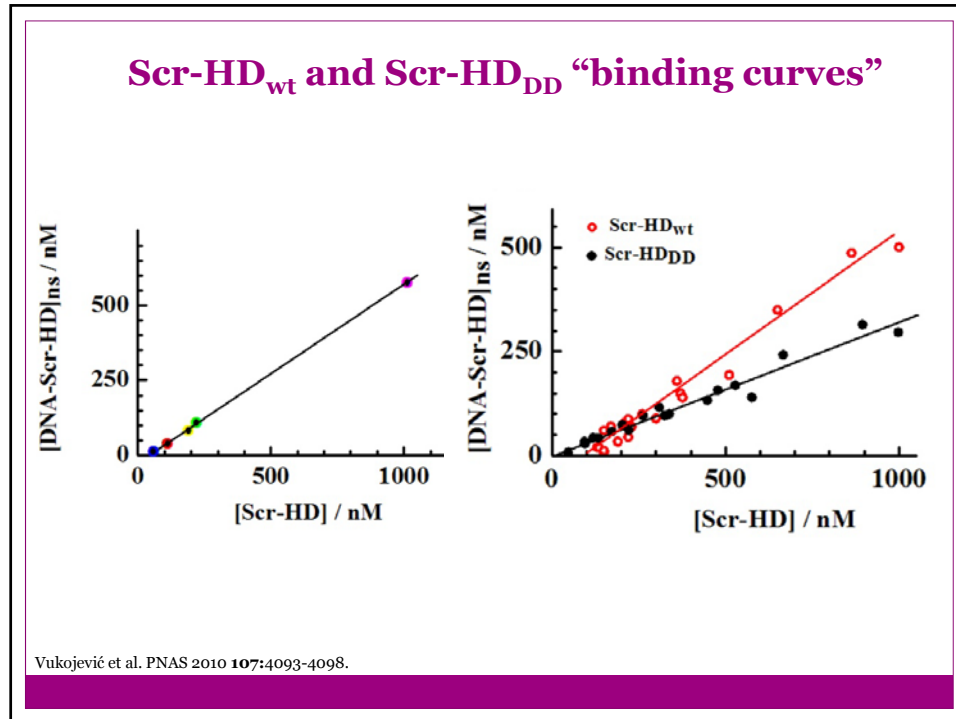
Fluorescence microscopy image of a Drosophila embryo showing Hox gene activity. The image is color-coded by Hox gene homology groups: 9-13 (Abd-B, red), 8 (abd-A, green), 1 (lab, blue), 4 (Dfd, orange), 5 (Scr, yellow), 6 (Antp, purple), and 7 (Ubx, pink).

<http://www.ncbi.nlm.nih.gov/bookshelf/br.fcgi?book=dbio&part=A1971>
http://scienceblogs.com/pharyngula/upload/2006/09/septuple_hox.jpg

Schematic representation of DNA-ScrHD_{wt} and DNA-ScrHD_{DD}. Both constructs show a DNA double helix with a binding site for the Scr transcription factor (red oval) and a poly-A tail (yellow line).







Estimation of the number of binding sites and dissociation constants

TAATCG or TAATGG

$$C_{\text{sites}}^{\text{non-specific}} = \frac{n}{V_{\text{nucleus}}} = \frac{1.94 \times 10^{-16}}{4.187 \times 10^{-12}} = 46 \mu\text{M}$$

$$C_{\text{sites}}^{\text{specific}} = \frac{n}{V_{\text{nucleus}}} = \frac{0.578 \times 10^{-18} \times 0.665}{4.187 \times 10^{-12}} = 92 \text{ nM}$$

$$K_d^{\text{ScrHD}_{DD}, ns} = (80 \pm 50) \mu\text{M}$$

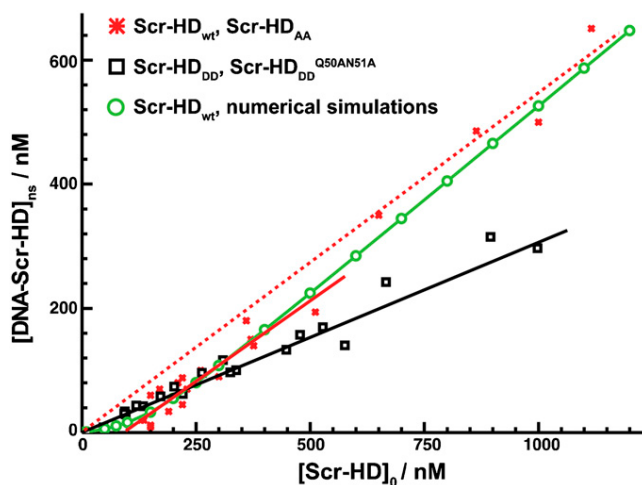
$$K_d^{wt,s} = (7 \pm 5) \text{ nM}$$

$$K_d^{wt,ns} = (25 \pm 15) \mu\text{M}$$

$$[(DNA - \text{ScrHD}_{wt})_s] = (80 \pm 50) \text{ nM}$$

Vukojević et al. PNAS 2010 **107**:4093-4098.

Simulation of Scr-HD binding to nuclear DNA



Vukojević et al. PNAS 2010 **107**:4093-4098.

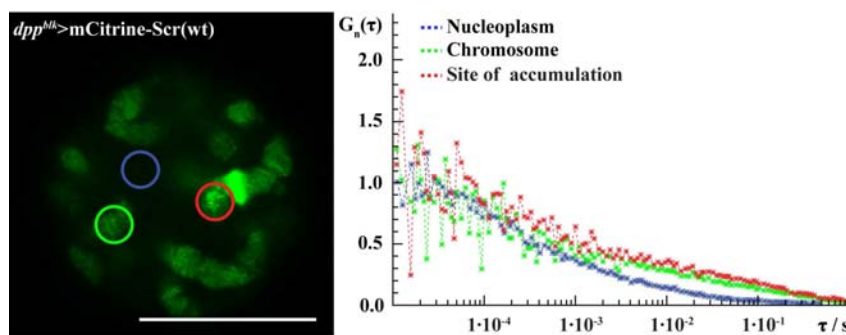
Iso-electric points for Scr-HD variants at different pH

pH	Charge			
	mCitrine-Scr-HD _{wt}	mCitrine-Scr-HD _{AA}	mCitrine-Scr-HD _{DD}	mCitrine-Scr-HD _{DD} ^{Q50AN51A}
7.00	7.2	7.2	5.2	5.2
7.10	6.4	6.4	4.4	4.4
7.20*	5.7	5.7	3.7	3.7
7.30*	5.1	5.1	3.1	3.1
7.40*	4.5	4.5	2.5	2.5
7.50*	4.0	4.0	2.0	2.0
7.60*	3.5	3.5	1.5	1.5
7.70*	3.1	3.1	1.1	1.1
7.80*	2.7	2.7	0.7	0.7
7.90*	2.3	2.3	0.3	0.3
8.00*	1.9	1.9	-0.1	-0.1
8.10*	1.5	1.5	-0.5	-0.5
8.20*	1.0	1.0	-1.0	-1.0
8.30	0.5	0.5	-1.5	-1.5
8.40	0.0	0.0	-2.0	-2.0
8.50	-0.5	-0.5	-2.5	-2.5
8.60	-1.1	-1.1	-3.1	-3.1
8.70	-1.8	-1.8	-3.8	-3.8
8.80	-2.6	-2.6	-4.6	-4.6
8.90	-3.4	-3.4	-5.4	-5.4

Iso-electric points estimated using the Protein Calculator v3.3
(<http://www.scripps.edu/cgi-bin/cdputnam/protcalc3>)

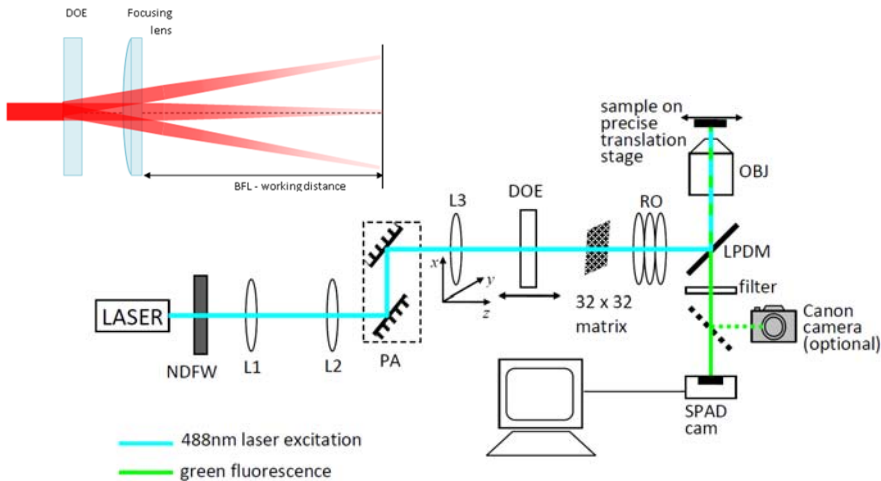
*Experimentally measured pH in salivary gland cells isolated from third instar larvae
(Schneider S., Wiinsch S., Schwab A., and Oberleithner H. (1996) Mol Cell Endocrinol 116, 73-79)

Limitations of single-point FCS



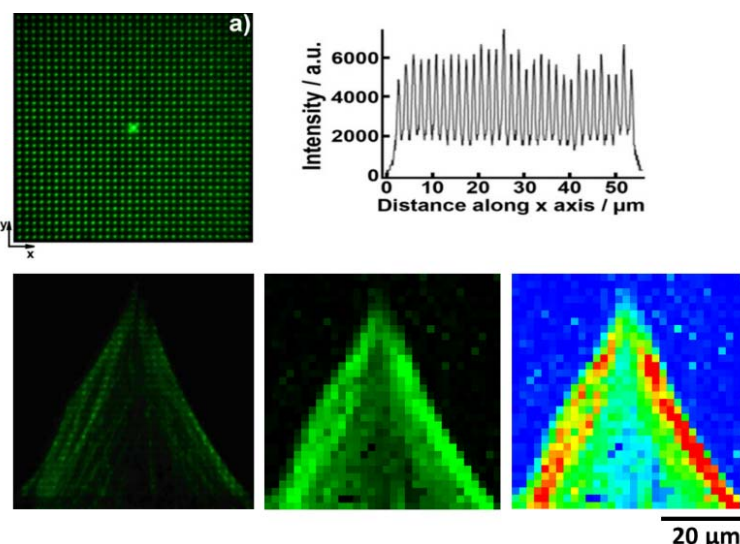
Vukojević et al. PNAS 2010 107:4093-4098.
Papadopoulos et al. Mech Dev. 2015 pii: S0925-4773(15)30029-0.

Overcoming the limited overview of classical FCS by massively parallel FCS



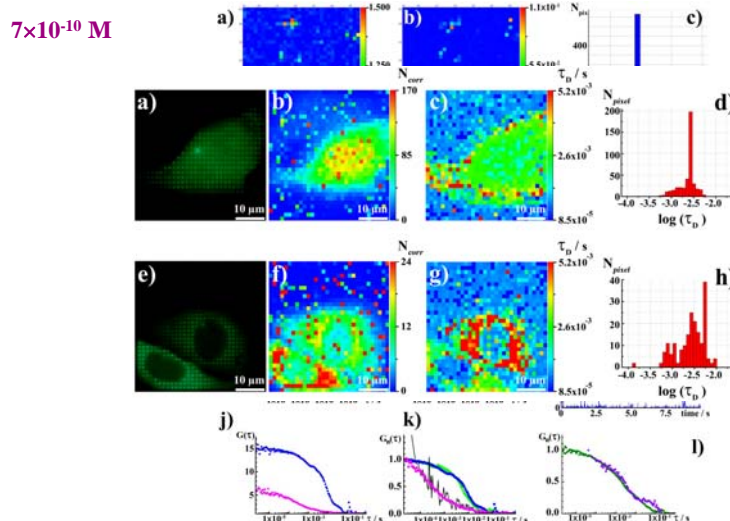
Vitali *et al.* IEEE J. Select. Topics Quantum Electron. 2014, *In press*
Krmpot *et al.*, submitted

Fast confocal imaging without scanning



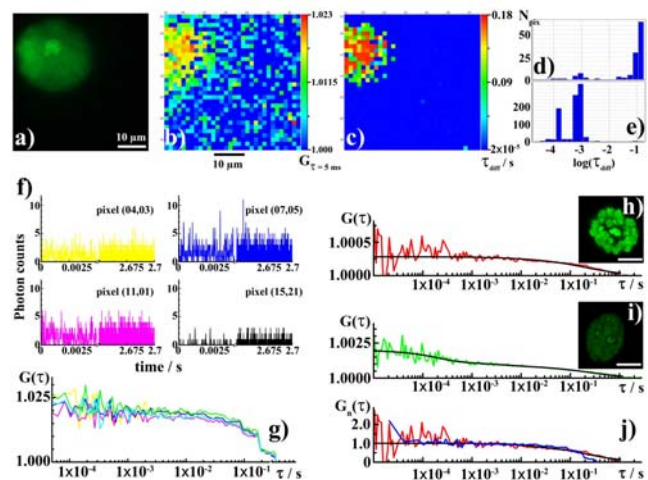
Krmpot *et al.* manuscript

Quantitative confocal fluorescence microscopy imaging of quantum dots in aqueous suspension



Krmpot et al. manuscript

Quantitative fluorescence microscopy imaging via massively parallel FCS



Krmpot et al. submitted

